

Design Optimisation of a Short Term Duty Electrical Machine for Extreme Environment

Puvan Arumugam, *Member IEEE*, Emmanuel Amankwah, Adam Walker, *Member IEEE* and Chris Gerada, *Member IEEE*

Abstract—This paper presents design optimisation of a short term duty electrical machine for extreme environments of high temperature and high altitudes. For such extreme environmental conditions of above 80° Celsius and altitudes of 30km, thermal loading limits are a critical consideration in machines, especially if high power density and high efficiency are to be achieved. The influence of different material on the performance of such machines is investigated. Also the effect of different slot and pole combinations are studied for machines used for such extreme operating conditions but with short duty. In the research, A Non-dominated Sorting Genetic Algorithm (NSGAII) considering an analytical electromagnetic model, structural and thermal model together with Finite Element (FE) methods are used to optimise the design of the machine for such environments achieving high efficiencies and high power density with relatively minimal computational time. The adopted thermal model is then validated through experiments and then implemented within the Genetic Algorithm (GA). It is shown that, generally, the designs are thermally limited where the pole numbers are limited by volt-amps drawn from the converter. The design consisting of a high slot number allows for improving the current loading and thus, significant weight reduction can be achieved.

Index Terms—Extreme Environment, optimisation, genetic algorithm, short-duty, thermal management

I. NOMENCLATURE

A	Current loading
B	Flux density
C_p	specific thermal heat capacity
E	Modulus elasticity
F	Force
I, I_p	Current, phase current
I_m	Moment of inertia
K_f	Copper packing factor
L	Conductor length
L_{ind}	Inductances

P	Pole number
P_t	Permeance
R	Resistances
N_{ph}, N_t	Number of turns per phase, Number of turns
T	Torque
T_{emp}	Temperature
V_r	Rotor volume
W_s, L_s	Weight and length of the shaft
W_r, L_r	Weight and length of the rotor
d_b	Stator bore diameter
d_r	Rotor diameter
e	Electromotive force
g	Gravity acceleration
f	Frequency
l_{stk}	Axial length
l_e	End winding length
l_g	Airgap
m	mass
S_{or}	Slot-opening ratio (slot width to slot-opening ratio)
S_t	Sleeve thickness
h_t	Tooth-tip height
h_m	Magnet height
t	Time
k_w	Winding factor
σ	Shear/normal stress
ω_c	Critical speed
α_t	Temperature coefficient
α	Magnet span

ABBREVIATION

OD	Outer diameter
SR	Spilt Ratio (d_b to OD ratio)
AR	Aspect ratio (d_r to l_{stk} ratio)
TR	Tooth width to slot pitch ratio
CW	Concentrated Winding
DW	Distributed Winding
PM	Permanent Magnet

II. INTRODUCTION

THE operation of electrical machines under extreme environments is becoming essential and the technologies to cope with such conditions are undergoing significant development [1, 2]. One of the extreme conditions is a high temperature environment where the performance and lifetime of the electrical machines are restricted due to both winding insulation properties and magnetic materials. This can be overcome through managing temperature within the machine which allows the machine to perform reliably. Alternatively,

Manuscript received December 22, 2016; revised March 30, 2017; accepted May 05, 2017.

Puvan Arumugam is with the Force Engineering Ltd, Shepshed, LE12 9NH, UK (e-mail: puvan@force.co.uk).

Emmanuel Amankwah is with Transmission Excellence Ltd, Kenilworth, Warwickshire, UK (email: Emmanuel@transmissionexcel.com).

Adam Walker and Chris Gerada are with the Power Electronics Machines and Control (PEMC) Group, University of Nottingham, UK and China (email:chris.gerada@nottingham.ac.uk).

materials that can endure the harsh operating conditions can be used but the overall performance will be compromised due to thermal effects and the poorer electrical or magnetic properties of such materials. Nevertheless, the performance can also be improved if the trade-offs between the electromagnetic, thermal and structural properties and associated material properties are considered in the early stage of the design [3-5].

Parametric analyses [6-8] is an effective method for the design of such machines, however, the method is timely expensive and it does not include the interaction between the design parameters. This further becomes unattractive when the multi-physics problem is considered. As an alternative, Genetic Algorithm (GA) which generate solutions to optimisation problems using techniques such as inheritance, mutation, selection and crossover, can be used for the design. The only identified drawback of GA is that the concept does not guarantee that an optimised solution will be found. However, use of GA is still a valuable design practice as it provides a multiple local optimum for a large number of parameters.

Numerous studies have been carried out on machine design optimizations using GA. In [9], an optimisation technique based on GA has been proposed for Surface Mounted Permanent Magnet (SPM) machines. In [10], a multi objective optimisation technique was used for Interior PM (IPM) machines to maximise the torque while achieving high frequency saliency to track the rotor position. Similarly in [11], a design methodology for an IPM machine utilising a zero-speed injection based sensor-less control has been investigated. In [12, 13], a Finite Element based multi-objective genetic algorithm has been adopted for IPM design in view of achieving maximum torque, minimum torque ripple, maximum flux weakening capability and minimum rotor harmonic losses. To minimize torque ripple and maximize the torque density, a bi-objective optimization of PM machine with parameter variables using Finite Element Analysis (FEA) and Differential Evolution (DE) has been employed in [14]. In [15], a multi-objective optimization of a SPM motor with five variables including the minimization of total weight and maximizing a goodness function (which is defined as torque per root square of losses at rated load) was studied. The comparison analysis between DE method and response surface method showed that DE has better capability dealing with large candidate designs. In [16], the optimisation via DE is further extended for eight variables with the objective of relative cost of active materials per cost. GA also was employed for optimising the shape of a magnetizer [17], the constant - power speed range [17] [18], salient-pole [19], fault-tolerance [20] and drive system [21, 22].

In [23], a filled function method (FFM) to find the global minimum of multi-modal and multidimensional functions has been introduced. In [24], multi objective Particle Swarm Optimisation (PSO) with a 2D finite element method was used to optimize complete machine design. In [25], the PSO was adopted with prediction error method (PEM) for identification of the actuator model of two-pole induction machine. Using PSO, the design of stress grading systems for large rotating machines was optimized in [26] where a system with up to eleven degrees of freedom were varied. An optimization on a

surface response [27], has been created to optimise the flux switching synchronous machine. In order to reduce the number of evaluations needed to construct the predictor, an adaptive method for the trial site selection was introduced as an improvement for the Latin Hypercube Sample (LHS) algorithm.

A numerical model based on FE method to gather using GA has also been used to reduce eddy current losses in permanent magnet electrical machines [28]. Similar concepts as in [28] have been implemented for minimisation of iron losses [29]. To minimise the computational effort of GA, Reluctance Network (RN) that allows to automatically generate the airgap RN and efficiently calculate the RN for any rotor position and any geometry variation of electrical machine has been proposed [30]. It was shown that the approach has a good numerical stability, and an accurate and fast computation through an optimization using the Jacobian method. A new heuristic approach for identifying induction motor equivalent circuit parameters based on experimental transient measurements from a vector controlled Induction Motor drive and using an off line Genetic Algorithm (GA) routine with a linear machine model has been studied in [31]. It was shown that accurate and fast estimation of the electrical motor parameters can be achieved. In [32], an optimisation for a high-speed PM machine designed for centrifugal air blower application has been done considering the multi-physics constraints, including the mechanical strength, rotor dynamics, mechanical losses, and thermal field. The use of analogue simulations and evolutionary algorithms for the sizing of complex actuator under multi-physic constraints has been investigated and report in [33]. Similarly, non-linear multi-physics analysis by means of finite-element method for an induction heating device has been carried out in [34], in which Pareto front was identified and then, compared with simplified linear analysis. Clearly, the use of GA for the optimum design of electrical machines has been well investigated for different purposes as illustrated by the broad spectrum of publications available in the literature. However, the use of GA for the design of machines for extreme environments under short duty operation are yet to be investigated.

In this paper, the use of Non-dominated Sorting Genetic Algorithm (NSGA-II) for the optimum design of a short time duty machine operating in extreme environment is investigated. A study case of 80°C and altitudes of 30km is considered in the design model although the conclusion applicable to other extreme environments of similar bearing on the machine operation. Of particular importance to the design is the choice of materials selected for the machine design, therefore the environmental constraints to meet the performance requirements of machines in such environments are gathered. A complete analytical environment is adopted within the NSGA-II and then used to investigate the possible slot and pole variants to meet the target operational performance. This allows predicting the electromagnetic, thermal and structural performances as well as interactions between them within a reduced time. As stated earlier, due to the short term duty operation of the machine, high thermal loading is expected and therefore, the accuracy of the thermal model is fundamental to optimum design of the machines. In

line with this objective, a model which represents the hot-spot temperature is developed and then, experimentally validated using a motorette. After, the model has been validated experimentally, the model is combined with an electromagnetic model and a structural model to perform the optimisation. Although the optimisation is completely based on analytical models, FE is however adopted for the final refinement of the design selected from Pareto front. The results show the performance comparison between the slot and the pole variants and how these influence the power density of the short duty machine. It is shown that the PM design is thermally limited wherein the pole numbers are limited by the volt-amps drawn from the converter. Interestingly, when the machine is designed with high slot numbers, the thermal loading improved and the heat dissipation is more effective and thus, high power density can be achieved. It is also shown that since the copper losses are the major loss component, use of a high saturation flux density material for the stator iron and a high conductivity material for the winding allow minimising the losses. Both the power density and the efficiency can therefore be improved. Finally, the design selection based on the performances and the manufacturing challenges involved in the design are detailed.

III. DESIGN REQUIREMENT AND CONCEPT SELECTION

The extreme environment presents a set of constraint on the design of the machine as well as the performance and efficiency expectations. The weight and the volume are the key design constraints which are dictated by the lack of available cooling and the short duty of the system. The design must also meet following constraints:

- the design envelope is limited to 200mm x 200mm x 200mm (length x width x depth);
- the power density should be higher than 16kW/kg;
- the design should provide maximum starting torque and high efficiency;
- the maximum converter DC link voltage should be less than 700V;
- the ambient temperature is over 80°C.

Since the power-density is a key design target, the design has to be traded between power-to-volume and power-to-weight. The machine must also be able to accelerate to speed within 1 second as the operational time is limited to 12 seconds. The machine is therefore ultimately designed to fulfil the performance while minimizing the overall size and weight together with reduced rotor mass.

From initial trade-off study between different candidate machines, it has been found that a PM solution which is thermally limited provides high power density [35, 36] compared to both an Induction Machine (IM) [37-39] and a Switch Reluctance Machine (SRM) [17, 40]. It is also seen that an IM is severely limited by magnetic saturation and thus, to achieve high performance the machine would have to be oversized or loaded with high current [41]. This results in poor efficiency performance. The SRM is the heaviest option due to the requirement of high peak torque. It is worth noting that the SRM has a significant torque ripple which also makes this topology unsuitable [42]. The PM is therefore selected for the design.

III. INITIAL CONSIDERATION ON OPERATIONAL ENVIRONMENT AND DESIGN MATERIAL

A way of achieving higher power density is through effective thermal management. In this design exercise, this fundamental concept is explored to achieve higher power densities of more than 16kW/kg in this extreme environments. Due to space limitation for applications in such high altitudes environments such as aerospace, a physical machine design envelope of 200mm x 200mm x 200mm cuboid is considered. A thermal ambience of 80°C which is not uncommon for such applications is set as the normal temperature for the machine operating environment. The other factors affecting the machine design are the supply voltage from the power electronics converter, - This is set to a maximum of 700V and the machine is also expected to deliver a high torque and faster acceleration.

In order to adopt high current loading and achieve a high power density, instead of Class H, enamelled copper magnet wire (rated to 180°C) or high-temperature versions of enamelled (polyimide) copper magnet wire (up to 245°C), stainless steel (e.g. Nickel) clad copper wire with ceramic fibre insulation is the most readily available option, with maximum operation temperatures up to 700°C, can be used [43]. But, due to the ceramic insulation, the minimum bend radius of this type of wire is large. This reduces the compactness of the end winding, consequently increasing the machine size. Also the stainless steel cladding introduces losses and requires welding for the electrical connection of the wire, rather than traditional means such as soldering. In addition, to perform the operation over 400°C, the ceramic insulator is required. This is because of other slot wall insulation material such as Kapton films and Nomex are limited up to 375°C. Due to higher insulation thickness of ceramic, the available slot area reduces, consequently it increases the winding losses.

Unlike the insulation material, the soft magnetic steels actually perform better at high temperatures as saturation flux density increases as a function of temperature and thus, the iron losses become lower. The key concern is the surface insulation of the steel which must be chosen to withstand the high temperatures. In contrast, the performance of the hard magnetic material is thermally limited, for example temperature rating of Neodymium-Iron-Boron is limited up to 250°C while Samarium Cobalt is up to 350°C. To withstand high temperature over 350°C, Alnico permanent magnets can be used instead, but due to their reduced remnant flux, the size is needed to be compromised to maintain similar performance.

Not only is the operational temperature an issue, the altitude at which the machine must operate is also a concern. Typically, a machine operated over an altitude of 1000 m experiences increased temperature as the ambient air has less cooling capacity. In addition, poor ventilation due to dirty or salty air also puts the machines lifespan at risk. Therefore an importance is initially given into material selection and maximum operational temperature.

IV. DESIGN OPTIMISATION

Fig.1 represents the process involved in the optimisation of the design. The optimisation is undertaken in four main steps:

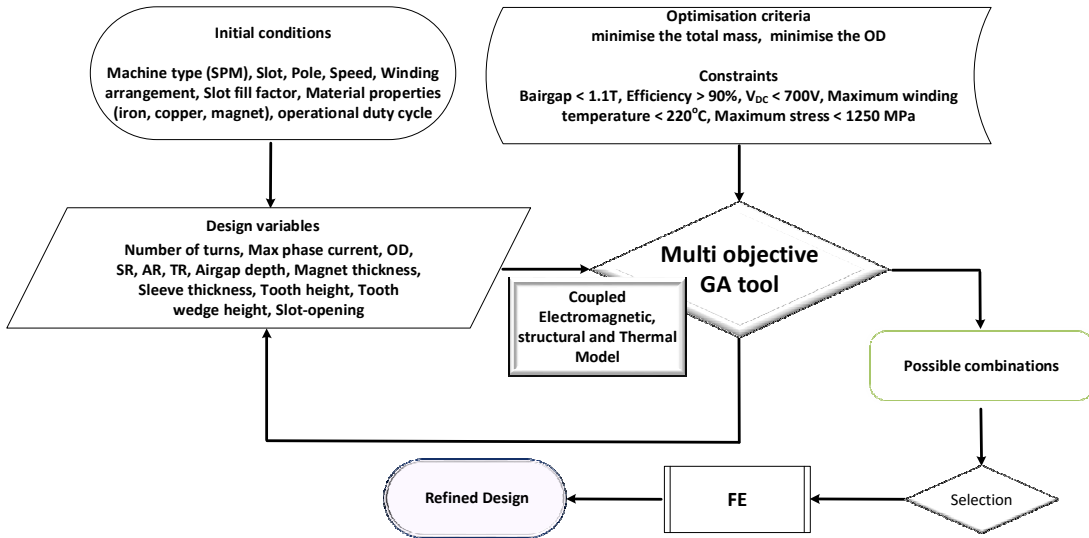


Fig. 1. Illustration of the design process

• The optimisation process starts with a Surface mounted PM machine with selected Slot (S) and Pole (P) combinations and associated winding arrangements. As illustrated in Fig.2, both Concentrated Winding (CW) and Distributed Winding (DW) arrangements are considered for different slot and pole selections in which the number of slots and pole are limited to 60 and 30 respectively. The choice of the Slot and Pole numbers have been selected considering the manufacturing difficulties involved when a high slot number is selected for a limited envelope and also because a high pole number introduces high switching losses in the converter.

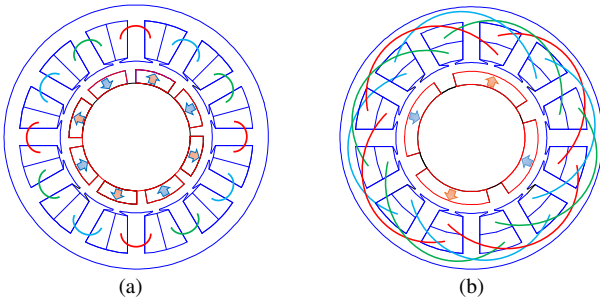


Fig. 2. Illustration of: (a) 12-slot 8-pole design with Concentrated Winding (CW) and (b) 12-slot 4-pole design with Distributed Winding (DW)

In the selection of the material for the design of the stator, Cobalt iron material is adopted due to its high saturation flux density. Specifically, Samarium Cobalt material which can withstand high temperature and also has a better reversible temperature coefficient than other similar materials available such as Neodymium-Iron-Boron is used for the PM machines design. To enhance the airgap flux density while allowing for the utilisation of both back-iron and shaft as a single solid body, a Halbach array magnet arrangement is adopted. For the winding material, the polyimide enamelled copper magnet wire (up to 245°C), is adopted along with Nomex slot insulator.

• In the second stage of the optimisation process, the machines physical design variables such as OD , SR , AR , TR , l_g , S_{or} , h_t , α , h_m , S_b , N_f and I_p are set within a range as in TABLE I.

 TABLE I
 DESIGN RANGE OF MACHINE PHYSICAL VARIABLE

Design Variable	Minimum	Maximum
OD	100mm	200mm
SR	0.4	0.7
AR	0.4	2
TR	0.3	0.75
l_g	0.5mm	3mm
S_{or}	0.05	1
h_t	0.25mm	7mm
α	0.3	0.9
h_m	3mm	20mm
S_b	1mm	15mm
N_f	1	1000
I_p	1A	700A

These design parameters are limited by the following constraints:

- no-load air gap flux density ≤ 1.1 T;
- efficiency $\geq 90\%$;
- maximum power requirement;
- converter voltage limit ≤ 700 V;
- maximum stress acting on the sleeve ≤ 1250 MPa;
- maximum hot spot winding temperature (T_{max}) \leq temperature of 220°C (with margin of 10%).

• In the third stage of the process, a multi objective genetic algorithm (GA) adopted for the optimisation process is implemented. The method used for the optimisation is a Non-dominated Sorting Genetic Algorithm (NSGAII) which was developed in [44]. As in other evolutionary algorithms, first the NSGA-II algorithm generates a random initial population which evolves during the optimisation process towards the global optimum. The key objective of the optimisation is to search for a designs that have maximum torque per kg and maximum torque per volume. These objective functions are evaluated for each individual criteria and then ranked. The offspring population is generated from the current population by selection, crossover and mutation. Finally, the process is repeated until the algorithm stops or a stopping condition (in this case a maximum number of iterations) is satisfied. The functionality of the optimisation tool can be found in detail in [44] and therefore not presented in this paper.

To avoid the geometry conflict due to the model parameters' dependency between themselves, an error routine is implemented within the optimisation. The error routine consists two set of procedures. First one limits the maximum and allows the maximum to be default when a geometry parameter exceeds the maximum value. For example, for an OD of 200mm, SR of 0.7, airgap of 1mm, sleeve thickness of 1mm and AR of 2, resultant axial length l_{stk} would be 276mm, but at this case the design takes the maximum default value of 200mm defined. This routine is also implemented for the slot opening. The second routine is used to prioritise the geometry parameter. For example when a rotor diameter is limited due to parameters such as SR, airgap and sleeve thickness, the envelope for both the magnet and the rotor back-iron may not be sufficient enough. In such cases the routine allows prioritising the magnet thickness over the back-iron depth. If the back-iron depth is less than defined minimal, the magnet thickness will be re-evaluated by taking into account default value for the back-iron. In a similar manner, the stator's geometry parameters are also handled. It is worth noting that the solution is defined to be null when the rotor geometry failed to satisfy the critical speed limit predicted by structural model.

A combined analytical model that predicts electromagnetic, thermal and structural performance of the machines is developed. For a successful evaluation of the analytical model, a number of assumptions are made, these include:

- the laminated steels has an infinite permeability;
- the slotting effects are neglected;
- only the fundamental winding factor harmonic is considered;
- iron losses due to localized saturations are neglected;
- slot fill factor of 0.5 is considered;
- high frequency effect on winding is not considered;
- demagnetization and localized stresses are neglected;
- there are no heat dissipation from the windings to the surrounding material.

Under above assumptions, the developed models are detailed in the following sub-sections.

A. Electromagnetic model

The fundamental relationship for torque production in PM machines is linked to Lorentz force in which the force F on a single conductor carrying a current I in a uniform magnetic field B can be expressed as [45]

$$F = B I L \quad (1)$$

If an electrical machine is considered to have N_{ph} conductors per phase carrying a current I and the windings are represented in an equivalent current sheet around the airgap perimeter, the linear current density A for a unit length can be described as:

$$A = \frac{3 N_{ph} I}{\pi d_b} \quad (2)$$

where d_b is stator bore diameter and factor 3 represents the number of phase windings. The force on the conductors can be expressed as a shear/normal stress σ [46]:

$$\sigma = \frac{F}{Area} = BA \quad (3)$$

where the flux density B is known as the magnetic loading and the linear current density A is also known as the electric loading. Since the machine has rotor diameter d_r and stack length of l_{stk} , the shear stress σ which produces a torque T can be written as:

$$T = F \frac{d_r}{2} = \sigma Area \frac{d_r}{2} = \frac{\sigma \pi d_r^2 l_{stk}}{2} = 2 V_r \sigma \quad (4)$$

where V_r is the rotor volume of the considered machine. Thus, equation (4) can be re-written as (5) [45].

$$T = 2 V_r B A \quad (5)$$

From (4) and (5), it is evident that the torque generated by the machine is proportional to the product of its rotor volume ($\propto d^2 l_{stk}$) and shear stress, where the shear stress is the product of the magnetic and electric loading. In the design, the electrical loading is restricted by factors such as the allowable slot area to accommodate the winding, the achievable packing factor of copper (K_f) in the stator slots, and the allowable packing copper current density based on the maximum allowable winding temperature rise. The magnetic loading is defined by both magnets' material properties and magnets' dimensions such as pole span and height. The magnetic loading is however limited by the saturation of the stator material used. Although the magnetic saturation is not considered in the model, it can be systematically included by knowing the properties of the stator material. Since the airgap flux density is known, the width of the stator tooth, and back iron thickness can be estimated by taking into account the saturation flux density at both stator tooth and back-iron. In parallel, the influence of the magnetic loading on current loading due to changes in the available slot area can also be calculated within the model.

To estimate the fundamental harmonic of the phase voltage, the back-emf (e) and voltage drop across active (*resistance* - R) and passive components (*inductance* - L and *drop across iron* - V_i) has to be calculated. These can be calculated from the following equations [46].

$$e = \frac{2 \pi f k_w N_{ph} B d_r l_{stk}}{\left(\frac{P}{2}\right)} \quad (6)$$

$$R = \frac{\rho(l_{stk} + l_e)}{A_s} \quad (7)$$

$$L = P_t N_{ph}^2 \quad (8)$$

where f is electrical frequency, k_w is the winding factor associated to the considered winding arrangement, l_e is the end winding length and ρ is resistivity of the conductive medium in the slot. P_t is the total permeance associated with both the geometry and the winding arrangement. To estimate the inductances accurately, the flux-leakage model based on the slot geometry [46] is adopted wherein tooth-tip and slot opening are accounted for. It is worth noting that the slotting effect is however not considered in the torque estimation. The iron losses are estimated based on Bertotti's equation by

averaging the flux density over a given area [47]. From these parameters, the resultant phase voltage is computed. Once the geometrical parameters associated with the design were predicted, the mass can be estimated based on the mass density of the material adopted. Once the whole electromagnetic performance is predicted, the losses obtained are fed into the thermal model, which is used to ensure the operation of the machine does not exceed the thermal limit, this is even more crucial when working which such a high current density machine.

B. Thermal model

As previously mentioned, the thermal hot-spot is expected to occur at the winding due to high torque density requirements for a given operational time. To assess this temperature rise within the winding a thermal model is therefore adopted. This makes a basic assumption that during the operation all the losses generated by the windings go towards increasing the windings temperature and it has linear characteristics within the considered time interval. It is thus assumed that there is no heat transfer from the windings to the surrounding magnetic material. This represents the worst-case thermal condition within the slot. Hence, based on the winding losses predicted by the electromagnetic model, the temperature rise within the slot domain can be expressed as follows:

$$T_{emp} = \int_{t_0}^{t_p} \frac{I_p^2 R_{i+1}}{m c_p} dt \quad (9)$$

where,

$$R_{i+1} = R_i (1 + \alpha_I (T_{emp_{i+1}} - T_{emp_i})) \quad (10)$$

where I_p is the phase current, m is the mass of the winding and c_p is the specific thermal heat capacity of copper. R_i is the initial resistance at the operating speed of the machine; T_{emp_i} is the initial temperature of the machine which is assumed equal to the ambient temperature (80° C) and α_I is the temperature coefficient of resistivity. Given that the machine is only under operation for a period of t_p , the final temperature of the machine (T_{emp_f}) can be re-written as

$$T_{emp_f} = \left[80 + \left(\frac{I_p^2 (R_i + R_i \alpha_I (T_{emp_f} - T_{emp_i}))}{m c_p} \right) \cdot t_p \right] ^\circ C \quad (11)$$

C. Structural model

Since the centrifugal force generates the significant stresses on the retaining sleeve as well as the magnets, selection of both the rotor diameter and the thickness of the sleeve have huge impact on the design. A large rotor diameter which increases the torque production requires an increased sleeve's thickness to withstand the centrifugal force. Increasing sleeve thickness results in an increased magnetic airgap which minimises the magnetic loading and thus, torque production. To include effectively these influences within the design, a structural model proposed in [48] is adopted. The adopted model calculates the minimal sleeve thickness for a given stress constraints by taking into account the rotor parameters. A safety margin of 20% is kept in the estimation of the sleeve thicknesses. The detailed model can be found in [48].

Critical speed is another structural constraint which determines the parameters of the rotor such as diameter and length. This is also influenced by the material used in the design. A formula given in (12) is therefore used to estimate the critical speed of the design wherein the material properties adopted for the design is used [49].

$$\omega_c = \frac{30}{\pi} \sqrt{\frac{g}{\left(\frac{5W_s L_s^3}{384E_s J} + \frac{W_r L_r^3}{484E_r J} \right)}} \quad (12)$$

where, g is gravity acceleration, J is moment of inertia, W_s , L_s , W_r , and L_r are weight and length of the shaft and the rotor respectively. E_s and E_r are modulus elasticity of the shaft and the rotor materials, respectively. Throughout the optimisation, the critical speed is kept 125% of the operational speed.

D. Experimental validation of thermal model

In order to obtain best design that has high power-to-weight and high power-to-volume, accuracy of the thermal model is important as it dictates the current loading for a given slot area. An experiment to validate the adopted thermal model within the design routine is therefore carried out using a motorette, which is a 6 slot section of a stator. The motorette was constructed with a traditional water jacket and a double layered distributed winding. The water jacket was used to return to starting temperatures after the test, not during the thermal increase. The copper was wound as if it were a 3 phase machine, but the ends of each phases were connected in series to allow for a single supply to power them all. The motorette, with water jacket and thermal insulation to the surface is shown in Fig.3.

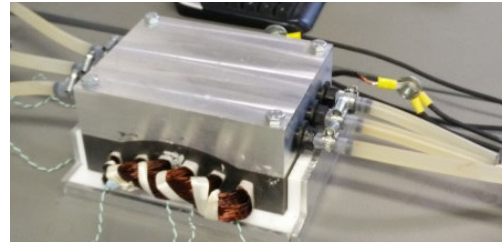


Fig. 3. A view of wound motorette

To increase the temperature in the windings a DC current was passed through the conductors. Using a DC current ensures the only losses are DC copper losses, which are easily and accurately calculable. This ensured that the total power converted to thermal energy was known exactly, which will be useful in later sections when the results were used to validate thermal models.

The windings were heated up to above the ambient of 80° C and allowed to cool back to this value. A short burst, greater than 10 seconds, of the desired current density was then applied. For each current density value the winding was allowed to cool back to 80° C and the current was applied again, this was cycled multiple times to ensure repeatability. The temperature was measured using thermocouples at various key spots, such as in the slot and the end windings. In the critical areas multiple thermocouples were used to obtain a temperature map, and to ensure the hot spot was observed. To

test the temperature increase, a range of current density values were used to give a spectrum of results. The results obtained are presented in Fig.4. The measured results under different current density clarify that regardless of amount of power losses, the heat generated due to the winding losses, is entirely accommodated within the slot for a period of time.

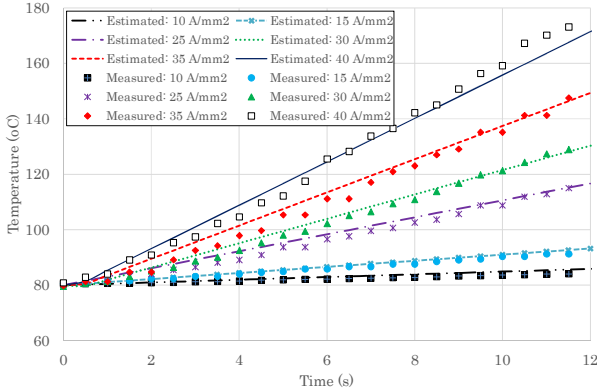


Fig. 4. Temperature rise for different current loading

While the losses of the thermal validation method would not match a full machine, the thermal pathways would. Often the downfall of thermal models is not the calculation of the losses but the overestimation of the conductivities, particularly in the slot. Under the model assumption on the generated heat due to copper losses, which is housed within the slot, the predicted temperature agrees well with the measured temperature. This clarifies that within the considered operational time the thermal conductivities between the slots to adjacent surface is negligible and thus, the heat transfer can be neglected – Validating the capability of adopted model in predicting the thermal characteristics of any slot geometry where the machine is under operation for a short time.

- The above developed analytical models are integrated within the GA optimisation tool to perform the optimisation by taking into account the influence of the each domain on the design. Once the optimisation routine is completed for a given slot and pole selection satisfying the constraints and criteria has been set, a design that has lower weight and volume is selected from the Pareto front [5] and then the selected candidate went through several stages of FE refinement where the influence of the saturation, slotting effects, inductance variation, MMF harmonics, winding arrangement and magnet demagnetization were considered.

V. RESULTS AND DISCUSSION

The population size for the differential evolution is 50 with a generation size of 200, which leads to a total of 10,000 designs. From the Pareto front, one optimized machine which has higher power density is selected for further refinement through a FE method.

Fig.5 shows the power density of the optimised machines at last generation. From the results, it can clearly be seen that although optimised designs provide the power density requirement while satisfying the design constraints requirements, the majority of the designs fail to satisfy the power density limit of 16kW/kg. Amongst qualified designs, A9 and B12 have the highest power density. It is worth noting

that though A9 has slightly less winding factor compared to variants A4, A5, A6, A8, A11, A12 and A13, it provides higher power density. This is mainly due to the thermal performances which dominate over the electromagnetic ones, where the design with high slot number has shown better performance. Since there are no significant heat transfer between slot and adjacent domains, high slot numbers facilitate reducing both the copper mass of a slot and the losses associated to those copper, consequently it reduces the temperature rise within the slot and allows for increased current loading. It is worth noting that though variant A11, A12 and A13 have high slot number, due to high pole numbers which restrict the electromagnetic performance, these provide reduced power density.

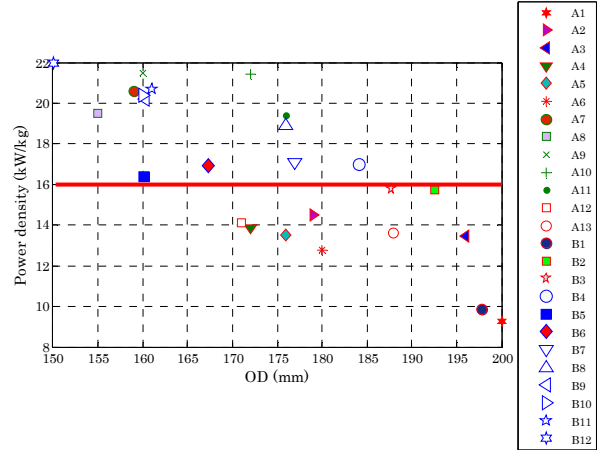


Fig. 5. Maximum power density of optimised different slot and pole variants (the notation of the associated slot and pole are given in Table II)

A. Influence of slot, pole and winding type

Table II details the performance of the considered slot and pole selections, where the designs meet same power requirements. From the results, it can be seen that amongst the designs, the 6-slot/4-pole is the heaviest solution. This is due to the low pole numbers and the low winding factor compared to other solutions. It can also be seen that the design cases are mostly limited by temperature; while a few cases, variants A11, A12, A13, B5 and B12, are electromagnetically restricted. Variants A11 to A13 consist of high pole numbers which limits the number of turns. As a result, it reduces the current loading as the maximum current is limited. So to achieve the torque required, the design needs to be oversized which ultimately adds the weight to the design. This is clearly evident in the solutions obtained for A11, A12, A13 and B5.

Though the higher pole number is expected to provide a higher torque, the design variant A6 (which has higher pole number than A5 for same slot number) provides a heavier solution. This is mainly due to a smaller slot per pole number compared to A5; consequently, it saturates the machine heavily than solution A5. This can further be seen from following groups which are concentrically wound: 9 slots with pole numbers 6 and 8; 12 slots with pole numbers 8, 10 and 14; 18 slots with pole numbers 12 and 16. In contrast, the distributed wound solution becomes lighter when the slot per pole number is smaller, for example: 18 slots with pole numbers 4 and 6; 24 slots with pole numbers 4 and 8; 36 slots with pole numbers 6, 8 and 12. This is mainly because of the

back-iron depth which becomes smaller with an increasing pole number. As a result, the volume and mass of the back-iron reduces. A similar observation can be made from the following slot per pole per phase groups: $q = 1$: 12 slot/4 pole, 18 slot/6 pole, 24 slot/8 pole and 36 slot/12 pole; $q = 1.5$: 18 slot/4 pole, 24 slot/6 pole and 36 slot/8 pole; $q = 2$: 24 slot/4 pole, 36 slot/6 pole, 48 slot/8 pole and 60 slot/6 pole.

TABLE II

PERFORMANCE COMPARISON BETWEEN OPTIMISED DESIGNS (A – CONCENTRATED WOUND MACHINE; B- DISTRIBUTED WOUND MACHINES)

Variant	S	P	q	N_{ph}	T_{emp} maximum	Efficiency (%)	Weight (pu)
A1	6	4	0.5	16	192	94.8	2.38
A2	9	6	0.5	15	184	94.3	1.52
A3	12	8	0.5	20	192	94.9	1.63
A4	9	8	0.375	15	195	94.8	1.59
A5	12	10	0.4	16	196	95.5	1.63
A6	12	14	0.285	16	156	94.7	1.72
A7	18	12	0.5	24	203	93.6	1.07
A8	18	16	0.375	18	183	94.7	1.13
A9	24	16	0.5	24	207	92.5	1.02
A10	27	18	0.5	27	203	94.0	1.03
A11	24	20	0.4	24	153	94.9	1.13
A12	24	22	0.363	16	138	95.8	1.56
A13	36	30	0.4	18	110	95.9	1.61
B1	6	4	0.5	16	185	93.9	2.23
B2	12	4	1	24	201	92.5	1.40
B3	18	4	1.5	24	210	92.5	1.39
B4	18	6	1	24	188	94.4	1.29
B5	27	6	1.5	18	197	94.0	1.34
B6	24	4	2	24	204	91.7	1.30
B7	24	8	1	24	200	94.8	1.29
B8	36	6	2	24	202	93.2	1.16
B9	36	8	1.5	24	202	93.7	1.09
B10	36	12	1	24	196	94.9	1.08
B11	48	8	2	24	206	93.7	1.06
B12	60	10	2	20	183	94.7	1.00

For the DW case, it is clear that the weight of the machine reduces with an increase in both slot and pole numbers. This explains that the solution which has high slot and pole number provides the performance with minimal mass. But, it is worth considering at the prototype stage that increasing the slot number introduces manufacturing challenges and cost as the available slot area reduces. In the CW case, similar trend can be seen, however increasing the number of slots and poles would not be effective due to electromagnetic constraints such as number of turns and the voltage limit from the converter.

B. Thermal aspects

Although the analytical thermal model does not consider the heat transfer between the windings and the surrounding bodies, this has been included in the refined final design via Motor-CAD thermal model [50]. Since the machine operation is within linear temperature region, use of the stator outer periphery as a casing allows minimizing the weight and thus, power-density can be improved. In the design, the machine is therefore considered to be enclosed as shown in Fig.6 where stator outer periphery serves as a casing. As can be seen in Fig.7, though the analytical model does not follow the same conditions as Motor-Cad model, it has similar characteristics within the considered operational interval. The hotspot temperature predicted by the Motor-Cad model starts to settle at 14 seconds whilst as expected the analytical model still has the linear characteristics.

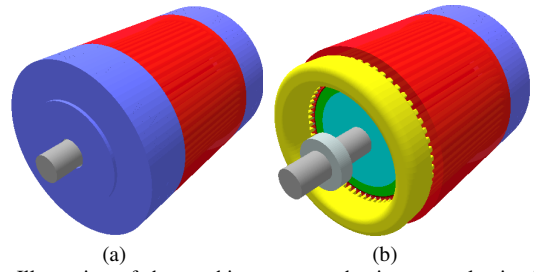


Fig. 6. Illustration of the machine structure having stator lamination as a casing (a) with end cap and (b) without end cap

From Fig.7, it is also worth highlighting that the higher slot number has very good thermal characteristics, with the hotspot temperature settling more quickly than the designs that consists of lower slot numbers. This is mainly due to the losses being distributed throughout the slot and the very good thermal path between slot and the back-iron. This is not the case for lower slot numbers in which the slot area is larger resulting in poorer heat removal. Given the performance requirement of high power-density, the initial design analysis indicates that both the 60-slot/10-pole design and 24-slot/16-pole design can be selected for the application. These two designs are further analysed by considering the material's influences on the power-density.

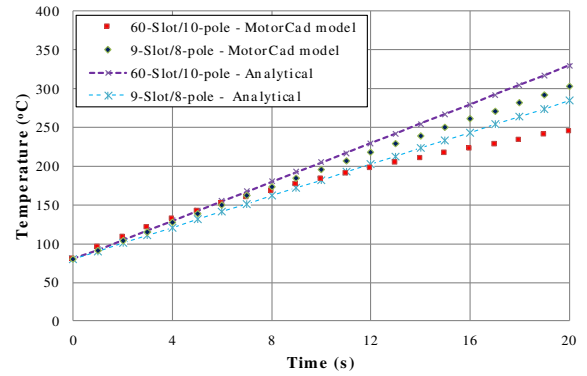


Fig. 7. Hotspot temperature comparison between analytically predicted and Motor-Cad model

VI. INFLUENCE OF THE MATERIAL ON DESIGN

Within this section, influences of the material selection on the design is investigated for two selected configurations: 24-slot/16-pole and 60-slot/10-pole.

A. Winding material

Instead Copper (Cu), aluminium (Al) is selected for winding and optimized for the designs, 24-slot/16-pole and 60-slot/10-pole. Due to low mass density, the design that includes aluminium as a winding material is expected to be lighter solution. In contrast, the higher resistivity of the aluminium requires larger slot area to reduce the losses and thus, accommodate the hot-spot winding temperature. The design parameters and the performances obtained are stated in Table III. It can be seen from the results that the design which includes aluminium has a heavier and bulkier solution. This is mainly due to the increase in the outer diameter to accommodate the losses. Clearly, the aluminium would be economical in terms of initial cost. However, it occupies more space and adds additional weights which make the solution unattractive.

TABLE III
PERFORMANCE COMPARISON BETWEEN SELECTED MACHINES WITH
DIFFERENT MATERIALS

Slot/pole	Material	Efficiency (%)	Weight (pu)
24/16	Cu	92.5	1.02
24/16	Al	95.1	1.54
60/10	Cu	94.7	1.00
60/10	Al	94.9	1.49
24/16	Vacoflux-50	92.5	1.02
24/16	JNHF	96.0	1.35
60/10	Vacoflux-50	94.7	1.00
60/10	JNHF	95.7	1.29

B. Type of steel

Initial selection for the design is Cobalt iron (Vacoflux-50, 0.3mm of lamination thickness). As an alternative Silicon steel (JNHF, 0.1mm of lamination thickness) is used for the stator and the designs are optimized accordingly. The adopted silicon steel has lower saturation flux density than Cobalt iron but it has lower losses under high frequency operation. So, it is expected to provide comprehensive performance. However, from the results in Table III clearly show that the Cobalt iron material allows the design to be smaller and lighter whilst Silicon steel requires increase tooth and back-iron area to avoid the heavy saturation. Consequently, Silicon steel reduces the active slot area and thus, to accommodate the thermal limit, the design has to be oversized. Since the power-density is a major design constraint, the Cobalt iron alloy is best candidate although the material is expensive.

In conclusion, both the 60-slot/10-pole design and 24-slot/16-pole design can be a good candidate for the application. Though these are feasible, these have pros and cons. The 60-slot/10-pole design has slightly less mass than the 24-slot/16-pole design, which can be further reduced if the end windings are wound effectively. Due to the distributed winding arrangement, the rotor has lower losses than the concentrated winding solution employed in 24/16 machine. In addition, the 60/10 design requires a lower PM mass than the 24/16 machine, but the initial stator manufacturing will be costly and challenging due to requirement of 60 slots. By contrast, the 24/16 machine design downsizes the cost and challenge, and improves the slot fill due to the windings which are wound only around a single tooth. This reduces the winding losses compared to the 60/10 solution. The key disadvantage of employing the 24/16 design is the operational frequency which is higher than the 60/10 machine solution. This would increase the switching losses associated with the converter counterpart, but on the other hand, it may reduce the harmonic losses associated with the machine. Considering the compactness of its winding and simplicity in the manufacturing, the 24/16 design is adopted for the further design prototyping.

VII. CONCLUSION

In this paper, an optimised design and analysis of a short-term electrical machine targeted for an extreme environment has been presented. A PM machine was selected and designed adopting integrated electromagnetic and thermal models within a NSGA-II optimisation tool. Via an experiment, it was shown that the adopted thermal model provides an accurate prediction of the temperature distribution within the machine windings. Then, the model was employed throughout the optimisation process together with electromagnetic model.

Integration of fully analytical tool within the NSGA-II optimisation routine enables the designs of wider slot and pole combination with relatively minimal amount of time. From the short duty designs, it is found that unlike the conventional machine design where the winding factor highly influences the design choice, the selection of the slot numbers improves the power density due to reduced thermal mass and losses associated with a slot which allows increasing the thermal load and thus, power density can be improved. It is also shown that high pole numbers are constrained due to the availability of volt-amp. For a given slot number, the concentrated wound solution becomes heavier when the slot per pole number reduces due to increase in the back-iron depth to avoid saturation. For a given slot or slot per pole per phase, the distributed wound solution becomes lighter when the slot per pole number is smaller as the back-iron depth reduces. Since the winding losses are major losses component, use of high conductive material for winding and high saturation flux density material for stator allows achieving improved power density.

REFERENCES

- [1] A. Boglietti, A. Cavagnino, A. Tenconi, S. Vaschetto, and P. d. Torino, "The safety critical electric machines and drives in the more electric aircraft: A survey," in *Industrial Electronics, 2009. IECON '09. 35th Annual Conference of IEEE*, 2009, pp. 2587-2594.
- [2] P. Arumugam and C. Gerada, "Short term duty electrical machines," 2016 XXII International Conference on Electrical Machines (ICEM), Lausanne, 2016, pp. 2676-2681.
- [3] G. D. Donato, F. G. Capponi, and F. Caricchi, "On the Use of Magnetic Wedges in Axial Flux Permanent Magnet Machines," *IEEE Transactions on Industrial Electronics*, vol. 60, pp. 4831-4840, 2013.
- [4] K. Kamiev, J. Montonen, M. P. Ragavendra, J. Pyrh, x00F, nen, *et al.*, "Design Principles of Permanent Magnet Synchronous Machines for Parallel Hybrid or Traction Applications," *IEEE Transactions on Industrial Electronics*, vol. 60, pp. 4881-4890, 2013.
- [5] A. Boglietti, A. Cavagnino, D. Staton, M. Shanel, M. Mueller, and C. Mejuto, "Evolution and Modern Approaches for Thermal Analysis of Electrical Machines," *IEEE Transactions on Industrial Electronics*, vol. 56, pp. 871-882, 2009.
- [6] K. G. Papadopoulos, C. Mademlis, A. M. Michaelides, C. P. Riley, N. Robertson, and I. Coenen, "Advanced parametric environment for electrical machines design optimization," in *Electrical Machines, 2008. ICEM 2008. 18th International Conference on*, 2008, pp. 1-6.
- [7] P. D. Pfister and Y. Perriard, "Very-High-Speed Slotless Permanent-Magnet Motors: Analytical Modeling, Optimization, Design, and Torque Measurement Methods," *IEEE Transactions on Industrial Electronics*, vol. 57, pp. 296-303, 2010.
- [8] N. Simpson, R. Wrobel, and P. H. Mellor, "A multi-physics design methodology applied to a high-force-density short-duty linear actuator," in *2014 IEEE Energy Conversion Congress and Exposition (ECCE)*, 2014, pp. 5168-5175.
- [9] N. Bianchi and S. Bolognani, "Design optimisation of electric motors by genetic algorithms," *IEE Proceedings - Electric Power Applications*, vol. 145, pp. 475-483, 1998.
- [10] N. Bianchi, D. Durello, and E. Fornasiero, "Multi-objective optimization of an Interior PM motor for a high-performance drive," in *Electrical Machines (ICEM), 2012 XXth International Conference on*, 2012, pp. 378-384.
- [11] J. Godbehere, R. Wrobel, D. Drury, and P. H. Mellor, "Design methodology of a brushless IPM machine for a zero-speed injection based sensorless control," in *2015 IEEE Energy Conversion Congress and Exposition (ECCE)*, 2015, pp. 5601-5608.
- [12] G. Pellegrino and F. Cupertino, "IPM motor rotor design by means of FEA-based multi-objective optimization," in *2010 IEEE International Symposium on Industrial Electronics*, 2010, pp. 1340-1346.
- [13] G. Pellegrino and F. Cupertino, "FEA-based multi-objective optimization of IPM motor design including rotor losses," in *2010 IEEE Energy Conversion Congress and Exposition*, 2010, pp. 3659-3666.
- [14] G. Y. Sizov, P. Zhang, D. M. Ionel, N. A. O. Demerdash, and M. Rosu, "Automated Multi-Objective Design Optimization of PM AC Machines Using Computationally Efficient FEA and Differential Evolution," *IEEE Transactions on Industry Applications*, vol. 49, pp. 2086-2096, 2013.
- [15] Y. Duan and D. M. Ionel, "A Review of Recent Developments in Electrical Machine Design Optimization Methods With a Permanent-Magnet Synchronous Motor Benchmark Study," *IEEE Transactions on Industry Applications*, vol. 49, pp. 1268-1275, 2013.
- [16] Y. Duan and D. M. Ionel, "Non-linear scaling rules for brushless PM synchronous machines based on optimal design studies for a wide range of power ratings," in

- 2012 IEEE Energy Conversion Congress and Exposition (ECCE), 2012, pp. 2334-2341.
- [17] M. Barcaro, N. Bianchi, and F. Magnussen, "Permanent-Magnet Optimization in Permanent-Magnet-Assisted Synchronous Reluctance Motor for a Wide Constant-Power Speed Range," *IEEE Transactions on Industrial Electronics*, vol. 59, pp. 2495-2502, 2012.
- [18] K. Kiyota, T. Kakishima, and A. Chiba, "Comparison of Test Result and Design Stage Prediction of Switched Reluctance Motor Competitive With 60-kW Rare-Earth PM Motor," *IEEE Transactions on Industrial Electronics*, vol. 61, pp. 5712-5721, 2014.
- [19] A. S. Bornschlegell, J. Pelle, S. Harmand, A. Fasquelle, and J. P. Corriou, "Thermal Optimization of a High-Power Salient-Pole Electrical Machine," *IEEE Transactions on Industrial Electronics*, vol. 60, pp. 1734-1746, 2013.
- [20] L. Papini, T. Raminosa, D. Gerada, and C. Gerada, "A High-Speed Permanent-Magnet Machine for Fault-Tolerant Drivetrains," *IEEE Transactions on Industrial Electronics*, vol. 61, pp. 3071-3080, 2014.
- [21] H. Gorginpour, H. Oraee, and R. A. McMahon, "Electromagnetic-Thermal Design Optimization of the Brushless Doubly Fed Induction Generator," *IEEE Transactions on Industrial Electronics*, vol. 61, pp. 1710-1721, 2014.
- [22] G. Lei, T. Wang, Y. Guo, J. Zhu, and S. Wang, "System-Level Design Optimization Methods for Electrical Drive Systems: Deterministic Approach," *IEEE Transactions on Industrial Electronics*, vol. 61, pp. 6591-6602, 2014.
- [23] X. Liu and W. Xu, "A Global Optimization Approach for Electrical Machine Designs," in *Power Engineering Society General Meeting, 2007. IEEE*, 2007, pp. 1-8.
- [24] M. v. d. Geest, H. Polinder, J. A. Ferreira, and D. Zeilstra, "Optimization and comparison of electrical machines using particle swarm optimization," in *Electrical Machines (ICEM), 2012 XXth International Conference on*, 2012, pp. 1380-1386.
- [25] S. Kiviluoto, Y. Wu, K. Zenger, and X. Z. Gao, "Identification of actuator model in an electrical machine by prediction error method and cultural particle swarm optimization," in *System Engineering and Technology (ICSET), 2011 IEEE International Conference on*, 2011, pp. 74-78.
- [26] C. Staubach, J. Wulff, and F. Jenau, "Particle swarm based simplex optimization implemented in a nonlinear, multiple-coupled finite-element-model for stress grading in generator end windings," in *Optimization of Electrical and Electronic Equipment (OPTIM), 2012 13th International Conference on*, 2012, pp. 482-488.
- [27] J. L. Duchaud, S. Hlioui, F. Louf, and M. Gabsi, "Electrical machine optimization using a kriging predictor," in *Electrical Machines and Systems (ICEMS), 2014 17th International Conference on*, 2014, pp. 3476-3481.
- [28] Z. Belli and M. R. Mekideche, "Optimization of magnets segmentation for eddy current losses reduction in permanent magnets electrical machines," in *Ecological Vehicles and Renewable Energies (EVER), 2013 8th International Conference and Exhibition on*, 2013, pp. 1-7.
- [29] M. Reinlein, T. Hubert, A. Hoffmann, and A. Kremser, "Optimization of analytical iron loss approaches for electrical machines," in *Electric Drives Production Conference (EDPC), 2013 3rd International*, 2013, pp. 1-7.
- [30] H. Nguyen-Xuan, H. Dogan, S. Perez, L. Gerbaud, L. Garbuio, and F. Wurtz, "Efficient Reluctance Network Formulation for Electrical Machine Design Using Optimization," *IEEE Transactions on Magnetics*, vol. 50, pp. 869-872, 2014.
- [31] K. Kampisios, P. Zanchetta, C. Gerada, and A. Trentin, "Identification of Induction Machine Electrical Parameters Using Genetic Algorithms Optimization," in *Industry Applications Society Annual Meeting, 2008. IAS '08. IEEE*, 2008, pp. 1-7.
- [32] Z. Huang and J. Fang, "Multiphysics Design and Optimization of High-Speed Permanent-Magnet Electrical Machines for Air Blower Applications," *IEEE Transactions on Industrial Electronics*, vol. 63, pp. 2766-2774, 2016.
- [33] F. Robert, F. V. D. Santos, C. Gutfrind, L. Dufour, and P. Dessante, "Multi-physics optimization of a smart actuator for an automotive application," in *Power Electronics and Applications (EPE'15 ECCE-Europe), 2015 17th European Conference on*, 2015, pp. 1-10.
- [34] P. D. Barba, I. Dolezel, M. E. Mognaschi, A. Savini, and P. Karban, "Non-Linear Multi-Physics Analysis and Multi-Objective Optimization in Electroheating Applications," *IEEE Transactions on Magnetics*, vol. 50, pp. 673-676, 2014.
- [35] M. v. d. Geest, H. Polinder, J. A. Ferreira, and M. Christmann, "Power Density Limits and Design Trends of High-Speed Permanent Magnet Synchronous Machines," *IEEE Transactions on Transportation Electrification*, vol. 1, pp. 266-276, 2015.
- [36] A. M. E.-. Refaie, J. P. Alexander, S. Galioti, P. B. Reddy, K. K. Huh, P. d. Bock, et al., "Advanced High-Power-Density Interior Permanent Magnet Motor for Traction Applications," *IEEE Transactions on Industry Applications*, vol. 50, pp. 3235-3248, 2014.
- [37] A. S. Abdel-Khalik, S. Ahmed, and A. M. Massoud, "Steady-State Mathematical Modeling of a Five-Phase Induction Machine With a Combined Star/Pentagon Stator Winding Connection," *IEEE Transactions on Industrial Electronics*, vol. 63, pp. 1331-1343, 2016.
- [38] A. S. Abdel-Khalik, M. A. Elgenedy, S. Ahmed, and A. M. Massoud, "An Improved Fault-Tolerant Five-Phase Induction Machine Using a Combined Star/Pentagon Single Layer Stator Winding Connection," *IEEE Transactions on Industrial Electronics*, vol. 63, pp. 618-628, 2016.
- [39] S. H. Kia, H. Heno, and G. A. Capolino, "Gear Tooth Surface Damage Fault Detection Using Induction Machine Stator Current Space Vector Analysis," *IEEE Transactions on Industrial Electronics*, vol. 62, pp. 1866-1878, 2015.
- [40] X. Ma, R. Su, J. Tseng King, S. Wang, X. Zhang, V. Vaiyapuri, et al., "Review of high speed electrical machines in gas turbine electrical power generation," in *TENCON 2015 - 2015 IEEE Region 10 Conference*, 2015, pp. 1-9.
- [41] E. B. Agamloh, A. Cavagnino, and S. Vaschetto, "Impact of Number of Poles on the Steady-State Performance of Induction Motors," *IEEE Transactions on Industry Applications*, vol. 52, pp. 1422-1430, 2016.
- [42] M. R. Feyzi, S. R. M. Aghdam, and Y. Ebrahimi, "A comprehensive review on the performance improvement in switched reluctance motor design," in *Electrical and Computer Engineering (CCECE), 2011 24th Canadian Conference on*, 2011, pp. 000348-000353.
- [43] L. Fang, I. Cotton, Z. J. Wang, and R. Freer, "Insulation performance evaluation of high temperature wire candidates for aerospace electrical machine winding application," in *2013 IEEE Electrical Insulation Conference (EIC)*, 2013, pp. 253-256.
- [44] K. Deb, A. Pratap, S. Agarwal, and T. Meyarivan, "A fast and elitist multiobjective genetic algorithm: NSGA-II," *IEEE Transactions on Evolutionary Computation*, vol. 6, pp. 182-197, 2002.
- [45] D. C. Hanselman, *Brushless Permanent-magnet Motor Design*: McGraw-Hill, 1994.
- [46] J. Pyrhonen, T. Jokinen, and V. Hrabovcova, *Design of Rotating Electrical Machines*: Wiley, 2009.
- [47] D. Eggers, S. Steentjes, and K. Hameyer, "Advanced Iron-Loss Estimation for Nonlinear Material Behavior," *IEEE Transactions on Magnetics*, vol. 48, pp. 3021-3024, 2012.
- [48] A. Binder, T. Schneider, and M. Klohr, "Fixation of buried and surface mounted magnets in high-speed permanent magnet synchronous motors," in *Industry Applications Conference, 2005. Fourth IAS Annual Meeting. Conference Record of the 2005, 2005*, pp. 2843-2848 Vol. 4.
- [49] "Kruger, "Technical Bulletin: TBN017.0/1998", [On Line]. Available: <http://www.ewp.rpi.edu/hartford/~ernesto/F2013/SRDD/Readings/Kruger-CriticalSpeeds-Shafts.pdf> [Accessed: September 2015]."
- [50] "Motor Design Limited, "About Motor Cad", [On Line]. Available: <http://www.motor-design.com/motorcad.php> [Accessed: October 2015]."



Puwan Arumugam (M'11) received the B.Eng. (Hons.) degree in electrical and electronic engineering from The University of Nottingham, Nottingham, U.K., in 2009, and the Ph.D. degree in electrical machines and drives from The University of Nottingham, Nottingham, U.K., in 2013. He subsequently worked as a researcher within the Power Electronics, Machines, and Control Group, The University of Nottingham, working on electric aircraft propulsion. He is currently a Senior Project Engineer with the Force Engineering Ltd, Shepshed, UK. His current research interests include electrical machines and drives, electromechanical devices and systems, and analytical computation of electromagnetic fields. Dr. Arumugam was awarded a Hermes Fellowship supported by Technology Transfer Office, The University of Nottingham in 2014.



Emmanuel Amankwah received the BSc degree in Electrical & Electronic Engineering from the KNUST Ghana (2006), MSc in Electrical Engineering (2009) and PhD Electrical & Electronic Engineering (2013) degrees from the University of Nottingham, Nottingham, UK. Emmanuel worked with the Electricity Company of Ghana (ECG) from 2006 to 2008 as a Design Engineer. After the PhD, he worked with the power electronics, machines and control research group at the University of Nottingham and is currently a Power Systems Consultant at Transmission excellence. His current research interests are power electronics in power systems, motor drive control and future power networks.



Adam Walker (M'15) received the Ph.D degree in electrical machines design from the University of Nottingham in 2017. He is currently working on an EPSRC Doctoral Prize project relating to electro-magnetic and thermal design of electrical machines and passives with the Power Electronics, Machines and Control Group at the University of Nottingham, UK. His main research interests are high performance traction machines, electrical machine thermal improvements and electro-magnetic design of passive devices.



Chris Gerada (M'05) received the Ph.D. degree in numerical modeling of electrical machines from The University of Nottingham, Nottingham, U.K., in 2005. He was subsequently a researcher with The University of Nottingham, where he was involved in high-performance electrical drives and the design and modeling of electromagnetic actuators for aerospace applications. Since 2006, he has been the Project Manager of the GE Aviation Strategic Partnership. In 2008, he was appointed as a Lecturer in electrical machines, an Associate Professor in 2011, and a Professor with The University of Nottingham, in 2013. His current research interests include the design and modeling of high-performance electric drives and machines. He serves as an Associate Editor of the IEEE Transactions On Industry Applications and is the Chair of the IEEE Industrial Electronics Society Electrical Machines Committee.